RAPID COMMUNICATIONS

PHYSICAL REVIEW B VOLUME 49, NUMBER 22 1 JUNE 1994-II

Long- versus short-range order in Ni_3V and Pd_3V alloys

C. Wolverton and Alex Zunger
National Renewable Energy Laboratory, Golden, Colorado 80401

Z.-W. Lu
Department of Physics, University of California at Davis, Davis, California 95616
(Received 18 January 1994; revised manuscript received 24 March 1994)

Measurements of the short-range-order (SRO) diffuse scattered intensity show peaks at the $\langle 1\frac{1}{2}0\rangle$ and $\langle 100\rangle$ points in Ni_3V and Pd_3V, respectively, although the stable ground state in both systems ($D0_{22}$) is a $\langle 1\frac{1}{2}0\rangle$-type structure. Mean-field theory predicts $\langle 1\frac{1}{2}0\rangle$ SRO in both materials, in contradiction with experiment for Pd_3V. The $\langle 100\rangle$-type SRO in Pd_3V has been explained previously as a non-mean-field effect. Via a combination of first-principles total-energy calculations and Monte Carlo simulated annealing, we show that non-mean-field effects are insufficient to explain the observed SRO of Pd_3V. However, the inclusion of electronic excitations leads to a temperature dependence in the interaction energies which correctly explains both the SRO and phase stability in Pd_3V and Ni_3V.

The isoelectronic alloys Ni_3V and Pd_3V both undergo an order-disorder transition between a low-temperature, long-range-ordered (LRO) $D0_{22}$ structure characterized by $\langle 1\frac{1}{2}0\rangle$ Bragg diffraction spots and a high-temperature disordered state. Experimental measurements[1,2] of short-range-order (SRO) diffuse scattered intensity in the disordered state have shown peaks at $\langle 1\frac{1}{2}0\rangle$ for Ni_3V, while surprisingly, Pd_3V exhibits peaks at the $\langle 100\rangle$ points, normally associated with $L1_2$-type LRO. This latter case is in direct contrast to the mean-field theory of SRO,[3] which equates the dominant wave vectors of SRO with those of the LRO.

This complete and qualitative failure of the mean-field theory was pointed out by Solal *et al.*,[2] who offered a non-mean-field (cluster variation method) explanation for the observed SRO in Pd_3V. These authors studied the problem in the context of an Ising model with first- and second-nearest-neighbor pair interactions, J_2 and K_2, showing that for J_2 and K_2 positive and $K_2/J_2 \ll 1$, there exists a "region" in which the LRO of the $\langle 1\frac{1}{2}0\rangle$ type can coexist with SRO peaking at $\langle 100\rangle$. In contrast, a mean-field solution to the same problem yields no such region. This non-mean-field region is illustrated in Fig. 1(a), in which the normalized SRO of type $\mathbf{k}$ is plotted as a function of the energy difference $\Delta E = E(L1_2) - E(D0_{22})$, normalized by J_2. The diffuse intensity due to SRO, was calculated here by Monte Carlo simulated annealing (to be described below). In Fig. 1(a), the non-mean-field region ranges between the vertical solid and dashed lines, and just as in the cluster variation calculation of Solal *et al.*,[2] the range of $0 < \Delta E/J_2 < +0.08$ affords the opportunity of $\langle 1\frac{1}{2}0\rangle$-type LRO coincident with $\langle 100\rangle$ SRO. The existence of such a region would appear to provide an explanation for the observation of $\langle 100\rangle$ SRO in Pd_3V in terms of non-mean-field behavior. However, first-principles, full-potential electronic structure calculations, based on the local density approximation (LDA), directly give the value of $\Delta E_{\rm LDA}$ (Ref. 4) for both materials, as shown in the first line of Table I. When these values are combined with the calculated values of J_2 for each system (details of these calculations to be given below), the values of $\Delta E_{\rm LDA}/J_2$ (third line of Table I) fall *well* outside the non-mean-field region [Fig. 1(a)] for both systems. To avoid the restriction of Solal *et al.* to two pair interactions, we have extended these calculations to include first- through fourth-nearest-neighbor pair [Fig. 1(b)] and triplet [Fig. 1(c)] interactions. Although the region in which mean-field theory fails may widen with these more extended interaction sets, still high precision LDA calculations place both M_3V systems well outside this range. Thus, accepting the $\Delta E_{\rm LDA}$ values, non-mean-field effects are insufficient to explain the observation of $\langle 100\rangle$ SRO in Pd_3V, as both Monte Carlo and mean-field give $\langle 1\frac{1}{2}0\rangle$ SRO for these values of $\Delta E_{\rm LDA}$.

We show here that the previously neglected finite-temperature electronic excitations reduce the energy difference between the $L1_2$ and $D0_{22}$ structures as temperature is increased. We present the results of calculated SRO for Ni_3V and Pd_3V from first-principles, total-energy LDA computations coupled with a simulated annealing calculation of the SRO, in which electronic excitations are included. These excitations, when coupled with a non-mean-field method for calculating the SRO, account for both the qualitative and quantitative detail of the experimentally observed SRO in both Ni_3V and Pd_3V.

To compute the SRO for the M_3V systems, we first define an Ising-like model, in which each atom of the alloy is assigned to the site of an ideal lattice (fcc, in this case), and the variable S_i is given the value $+1$ (-1) if an A (B) atom is assigned to site i. Within this description, the energy of any configuration of atoms (denoted by σ) can be written in a cluster expansion (CE):[5]

$$E_{\rm CE}(\sigma) = \sum_f D_f J_f \bar{\Pi}_f(\sigma) \ , \qquad (1)$$

where f is a figure comprised of several lattice sites (pairs, triplets, etc.), D_f is the number of figures per lattice site, J_f is the Ising-like interaction for the figure f, and $\bar{\Pi}_f$ is a function defined as a product over the figure f of the variables S_i, averaged over all symmetry equivalent figures of lattice sites.

In this paper, we calculate J_f using the "total-energy inversion method"[6] in which a set of total energies $\{E_{\rm LDA}\}$ is used to fit a smaller set of interactions energies, $\{J_f\}$. We use fully relaxed, linearized augmented plane wave (LAPW) calculations and unrelaxed, linear muffin-tin orbital (LMTO) calculations to obtain the interaction parameters for Ni-V and Pd-V, respectively. For Ni-V (Pd-V), we have used 24 (18) structures and 12 (14) interactions in the fit. We include pair figures

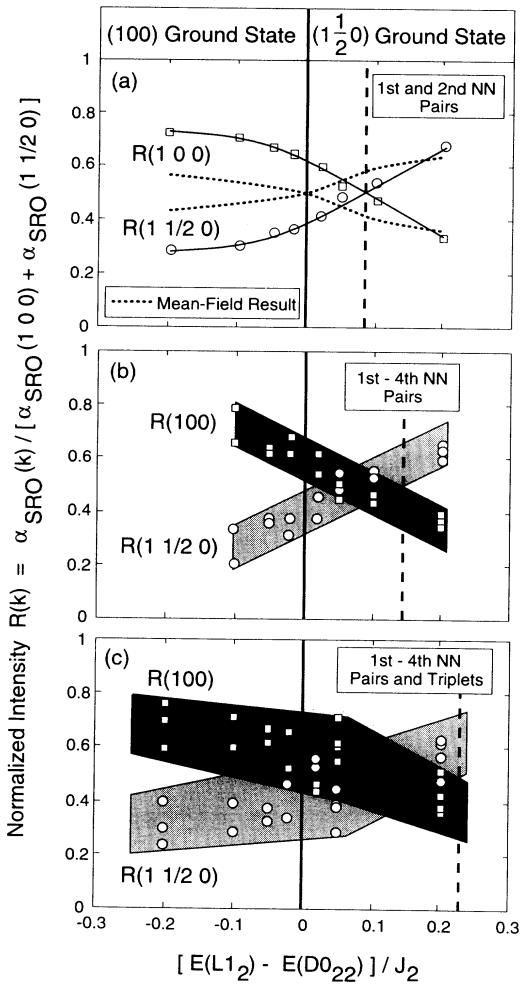

FIG. 1. Model calculations of the normalized SRO intensity $R(\mathbf{k})$ as a function of $\Delta E/J_2$ with (a) first- and second-neighbor pair, (b) first- through fourth-neighbor pair, and (c) first- through fourth-neighbor pair and triplet interactions. The squares and circles indicate the Monte Carlo results for $R(100)$ and $R(1\frac{1}{2}0)$, respectively. In (b) and (c), the interactions were chosen at random such that no interaction (except J_2) have magnitude greater than $0.2J_2$ and all interaction sets have as ground states either $L1_2$ or $D0_{22}$. The vertical solid (dashed) lines delineate $\langle 1\frac{1}{2}0\rangle$ from $\langle 100\rangle$ LRO (SRO).

TABLE I. $T = 0$ K total energy differences ($L1_2$ minus $D0_{22}$) as given by direct LAPW calculations ($\Delta E_{\rm LDA}$) and by the cluster expansions described in the text ($\Delta E_{\rm CE}$). All energies are in meV/atom. The LAPW calculated densities of states at the Fermi level, n_F, are given for the $L1_2$ and $D0_{22}$ structures in $(\mathrm{Ry})^{-1}\mathrm{atom}^{-1}$, as are the coefficients of Eq. (5), $A_{\rm fit}$ and $A_{\rm Somm}$. Monte Carlo (MC) calculated and experimental transition temperatures are given in degrees Kelvin.

Quantity	Ni_3V	Pd_3V
$\Delta E_{\rm LDA}$ $(T = 0$ K)	+105.1	+71.5
$\Delta E_{\rm CE}$ $(T = 0$ K)	+103.3	+58.2
$\Delta E_{\rm LDA}/J_2$ $(T = 0$ K)	+4.1	+4.3
$n_F(L1_2)$	40.70	40.00
$n_F(D0_{22})$	7.78	11.88
$A_{\rm fit}$	−54.4	−50.1
$A_{\rm Somm}$	−54.2	−46.2
ΔF $(T = T_{\rm calc})$	+17.5	−7.5
$T_c^{\rm calc}$ $(A = 0)$	1900	1600
$T_c^{\rm calc}$ $(A = A_{\rm fit})$	1400	1250
T_c (expt)	1318[a]	1088[a]

[a]Reference 8.

which extend to the fourth-nearest-neighbor fcc distance, as well as triplet and quadruplet figures. The CE values, $\Delta E_{\rm CE}$, (second line of Table I) compare favorably with the LDA energies $\Delta E_{\rm LDA}$ (first line of Table I).

The interactions are used in Eq. (1) in conjunction with Monte Carlo simulated annealing.[7] This gives (i) the $T = 0$ K ground state structures (from a simulation of a finite-size cell at a temperature where all configurational changes proved to be energetically unfavorable), (ii) the SRO and (iii) the order-disorder transition temperature, T_c. We use a system size of $16^3 = 4096$ atoms with periodic boundary conditions.

We find for both Ni_3V and Pd_3V that the $T = 0$ K ground state structure is $D0_{22}$, in agreement with the experimentally assessed[8] phase diagrams. The Warren-Cowley SRO parameter for the nth atomic shell is

$$\alpha_{\rm SRO}(n) = (\bar{\Pi}_{0,n} - q^2)/(1 - q^2)\ , \qquad (2)$$

where $q = 2x - 1$. The Fourier transform of Eq. (2), $\alpha_{\rm SRO}(\mathbf{k})$, is calculated using 500 Monte Carlo steps to equilibrate the system and subsequently, averages are taken over 50 Monte Carlo steps. Twenty atomic shells of $\alpha_{\rm SRO}(n)$ are used in the calculations of Fig. 1, whereas 35 and 10 shells are used for Ni_3V and Pd_3V, respectively, these latter two cases being dictated by the number of experimental SRO parameters reported. As can be expected from Fig. 1, our Monte Carlo calculated SRO, $\alpha(\mathbf{k})$, using the LDA determined interaction energies J_f produces $\langle 1\frac{1}{2}0\rangle$ peaks, consistent (via mean-field theory) with the ground state symmetry, but in conflict with the experimental SRO for Pd_3V. The changes required in $\Delta E_{\rm LDA}$ to obtain the correct SRO symmetry are well outside our computational errors. Furthermore, all effects of a configurational nature, (long-range order, short-range order, configurational entropy) have been accounted for properly in the Monte Carlo simulations and hence are

already accounted for in the non-mean-field region of Fig. 1. These configurational excitations, therefore, *may not* serve as the resolution to the contradiction, but rather, some excitation which does not change the configuration must be explicitly addressed.

The inability of the LDA-based CE to produce the experimentally observed SRO for Pd_3V may be resolved by realizing that the LDA energies (and hence, the sets of J_f) are pertinent to $T = 0$ K, while the SRO is necessarily measured at a temperature above the order-disorder transition. One temperature-dependent effect which is not configurational in nature is the free energy associated with electronic excitations. According to the Sommerfeld theory, the electronic energy $U_{\rm el}$ and entropy $S_{\rm el}$ at temperatures low compared with the Fermi temperature (as in the SRO experiments) are quadratic and linear functions of temperature, respectively, and in particular, the differences of these two quantities between the $\langle 100\rangle$-type $L1_2$ and $\langle 1\frac{1}{2}0\rangle$-type $D0_{22}$ structures are given by

$$\Delta U_{\rm el}(L1_2 - D0_{22}; T) = (\pi^2/6)k_B^2 T^2 \Delta n_F \ , \qquad (3)$$

$$\Delta S_{\rm el}(L1_2 - D0_{22}; T) = (\pi^2/3)k_B^2 T \Delta n_F \ ,$$

where $\Delta n_F = n_F(L1_2) - n_F(D0_{22})$ is the difference in densities of states (DOS) at the Fermi level, E_F, between the $L1_2$ and $D0_{22}$ structures. The $T = 0$ K energy difference $\Delta E_{\rm CE}$ between $L1_2$ and $D0_{22}$ is now replaced by the temperature-dependent difference

$$\Delta F(T) = \Delta E_{\rm CE} + [\Delta U_{\rm el} - T\Delta S_{\rm el}] \ . \qquad (4)$$

Thus, if the two structures have significantly different DOS at E_F [with $n_F(L1_2) > n_F(D0_{22})$], their energy difference $\Delta F(T)$ will be much smaller at high T (where SRO is measured) than at low T (where the ground state is determined). The densities of states at the Fermi level as calculated from LAPW are listed in Table I for both $L1_2$ and $D0_{22}$. In most cases, different structures of the same composition have comparable DOS at E_F. However, there is a huge disparity between $n_F(L1_2)$ and $n_F(D0_{22})$, leading to a significant electronic free energy [Eq. (4)] at high T.

We wish to determine, in the spirit of a model calculation whether electronic excitation effects could explain the qualitative failure of $T = 0$ cluster expansions to reproduce the correct $\langle 100\rangle$-type SRO symmetry seen in Pd_3V. To do so, we parametrize Eqs. (3) and (4) as

$$\Delta F(T) = \Delta E_{\rm CE} + A(k_B T)^2 \qquad (5)$$

and equate this with a cluster expansion in the form of Eq. (1). Electronic excitations thus lead to temperature-dependent interactions

$$J_f(T) = J_f(0) + A_f(k_B T)^2 \ . \qquad (6)$$

(Note that *configurational* excitations do not lead to temperature-dependent interactions.) We choose to project the temperature dependence only onto the interactions which are the most sensitive to the relevant energy differences of the problem, $\Delta E(L1_2 - D0_{22})$ and the ordering energy of $D0_{22}$. With this criterion, the temperature dependence is included in a three- and four-body interaction, J_3 and K_4, respectively.[9] Using Eq. (6), we first fit the observed SRO by adjusting the constant $A = A_{\rm fit}$ in Eq. (5). We will then contrast $A_{\rm fit}$ with its *ab-initio* value, $A_{\rm Somm} = (-\pi^2/6)\Delta n_F$ from the Sommerfeld formula [Eq. (3)], using LDA calculated densities of states, n_F.

The calculated and experimental[1,2] SRO for Ni_3V and Pd_3V are shown in Figs. 2 and 3, respectively. For both alloys, the calculated SRO is shown both without and with the effect of electronic excitations [i.e., with $A = 0$ and $A = A_{\rm fit}$ of Eq. (5)]. For Ni_3V, both calculations show peaks at the $\langle 1\frac{1}{2}0\rangle$ points, in qualitative agreement with the neutron diffraction[1] data. The intensities of the calculated $\langle 1\frac{1}{2}0\rangle$ peaks are 8.5 and 4.1 without and with electronic excitations, to be compared with the experimental value of 4.2. Thus, only when these excitations significantly reduce the $T = 0$ value of $\Delta E_{\rm LDA}$ does one obtain a good *quantitative* agreement between calculated and experimental SRO intensities. At high temperatures, the energy $\Delta F(T)$ eventually changes sign. Thus, the calculation of the Ni_3V SRO with electronic excitations shows a shift of the peak position from the $\langle 1\frac{1}{2}0\rangle$ to $\langle 100\rangle$ points as temperature is increased. Also, with the same values of $J_f(T)$ used to calculate the Ni_3V SRO, we are able to quantitatively reproduce the measured[1]

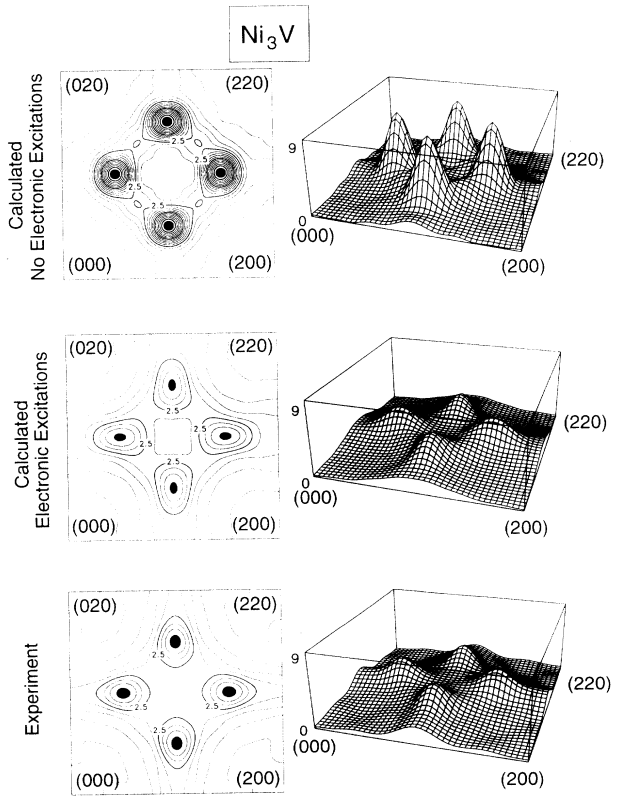

FIG. 2. Experimental (Ref. 1) and Monte Carlo simulated annealing calculated values of $\alpha_{\rm SRO}(\mathbf{k})$ for Ni_3V in the $(hk0)$ plane. The black shading in the contour plots locates the peaks in the SRO pattern.

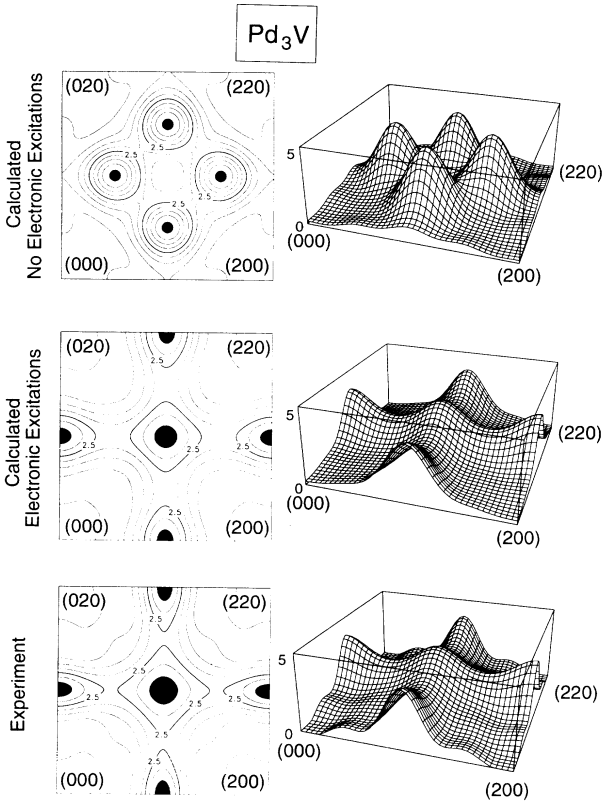

FIG. 3. Experimental (Ref. 2) and Monte Carlo simulated annealing calculated values of $\alpha_{\mathrm{SRO}}(\mathbf{k})$ for Pd_3V in the $(hk0)$ plane. The black shading in the contour plots locates the peaks in the SRO pattern.

SRO of Ni_2V. For Pd_3V, the calculation without electronic excitations show large peaks at the $\langle 1\frac{1}{2}0\rangle$ points, in qualitative conflict with the neutron diffraction[2] data. [Recall that this discrepancy is to be expected based on the large value of $\Delta E_{\mathrm{LDA}}/J_2$ (Table I) which falls well outside the non-mean-field region of Fig. 1.] Thus, for Pd_3V, the temperature dependence of Eq. (5) is necessary to produce calculated SRO in both qualitative and quantitative agreement with the experimental SRO. The strengths of the calculated $\langle 100\rangle$ peaks are 1.0 and 3.7 (without and with temperature-dependent interactions), compared with the experimental value of 3.8, while for the $\langle 1\frac{1}{2}0\rangle$ peaks 4.6 and 2.3 are the calculated values, and 2.5 is that of neutron diffraction.

The values of the fitted A are compared in Table I with the *ab-initio* Sommerfeld values, and for both alloys, the comparison is quite favorable. Table I also shows that electronic excitations (using A_{fit}) lower $\Delta E(T=0)$ significantly: at the calculated temperatures of the SRO, we have $\Delta F = 19.3$ meV/atom for Ni_3V and -7.5 meV/atom for Pd_3V, compared with the $T=0$ values $\Delta E_{\mathrm{CE}} = +103.3$ and $+58.2$, respectively. As stated previously, this energy lowering is in addition to any configurational (LRO,SRO) temperature dependence. Hence, this leads us to the main conclusion of this work: *electronic excitations lower sufficiently the energy of $L1_2$ relative to $D0_{22}$ so that the SRO wave vector changes from $\langle 1\frac{1}{2}0\rangle$ to $\langle 100\rangle$ for Pd_3V alloys.*

It is interesting also to note the effect of these excitations on the transition temperature, T_c. Experimental and Monte Carlo calculated values of T_c are given in Table I. The electronic excitations have a dramatic effect, lowering the calculated transition temperatures by 350–500 K, thereby bringing both temperatures within 100–200 K of the experimentally assessed values.

Our main results can be summarized as follows. (i) Our Monte Carlo calculations confirm the cluster variation method results of Solal *et al.* to the effect that there is a range of first- and second-neighbor interactions in which $\langle 1\frac{1}{2}0\rangle$-type LRO can coexist with $\langle 100\rangle$-type SRO. (ii) This *does not* solve the problem of Pd_3V [which exhibits experimentally $\langle 1\frac{1}{2}0\rangle$-type LRO and $\langle 100\rangle$-type SRO], since accurate LDA calculations place the parameters of these materials *well outside* the above range. (iii) While inclusion of more distant neighbor interactions broadens the parameter range in which $\langle 1\frac{1}{2}0\rangle$-type LRO can coexist with $\langle 100\rangle$-type SRO, still Pd_3V falls well outside this range. Hence, non-mean-field effects are insufficient to explain the wave vector symmetry of the Pd_3V SRO. (iv) Finite temperature electronic excitation effects, which are proportional to the *difference* in Fermi level densities of states between the $L1_2$ and $D0_{22}$ structures, lead to a large effective reduction of $\Delta E/J_2$. (v) This reduction leads not only to the correct predicted symmetry of the calculated SRO, but also to quantitative agreement with experimentally assessed SRO intensities and transition temperatures in quantitative agreement with the experimentally assessed phase diagrams.

Work at NREL was supported by the Office of Energy Research (OER) [Division of Materials Science of the Office of Basic Energy Sciences (BES)], U.S. Department of Energy, under Contract No. DE-AC-02-83-CH10093.

[1] R. Caudron, M. Sarfati, M. Barrachin, A. Finel, F. Ducastelle, and F. Solal, J. Phys. I (France) **2**, 1145 (1992); A. Finel (private communication).

[2] F. Solal, R. Caudron, F. Ducastelle, A. Finel, and A. Loiseau, Phys. Rev. Lett. **58**, 2245 (1987).

[3] M. A. Krivoglaz and A. A. Smirnov, *The Theory of Order-Disorder in Alloys* (McDonald, London, 1964); P. C. Clapp and S. C. Moss, Phys. Rev. **142**, 418 (1966).

[4] Previous LMTO calculations employing the atomic-sphere approximation for Ni_3V [W. Lin, J. H. Xu, and A. J. Freeman, Phys. Rev. B **45**, 10 863 (1992), and references therein] all give values of ΔE_{LDA} which are within several meV/atom of one another, and also agree well with our full-potential results.

[5] J. M. Sanchez, F. Ducastelle, and D. Gratias, Physica A **128**, 334 (1984).

[6] A review is given in A. Zunger, in *Statics and Dynamics of Alloy Phase Transformations*, edited by P. E. A. Turchi and A. Gonis, NATO ASI Series (Plenum, New York, 1994).

[7] Z.-W. Lu, D. B. Laks, S.-H. Wei, and A. Zunger (unpublished).

[8] J. F. Smith, in *Phase Diagrams of Binary Vanadium Alloys* (ASM International, Metals Park, OH 1987).

[9] J_3 has coordinates (000), (110), and (101), while K_4 has coordinates (000), (110), (101), and (200).

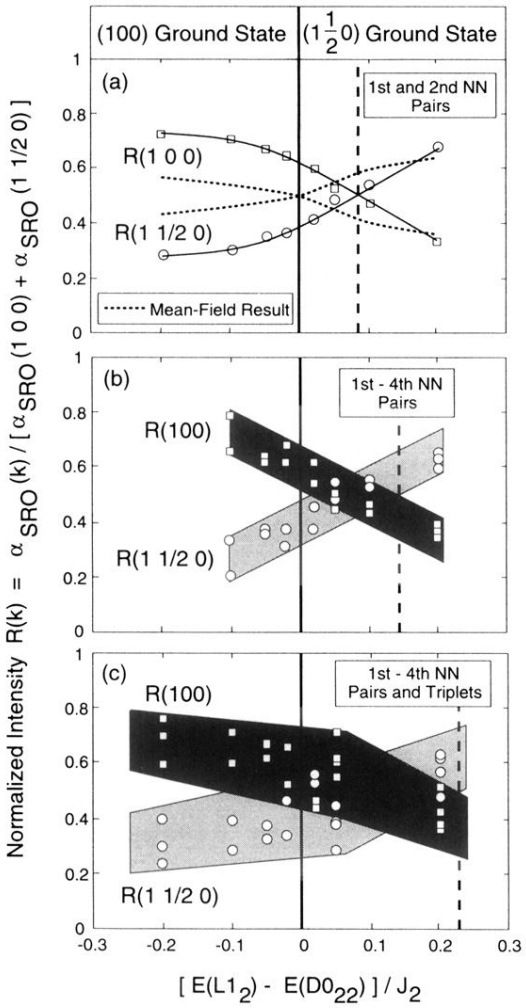

FIG. 1. Model calculations of the normalized SRO intensity $R(\mathbf{k})$ as a function of $\Delta E/J_2$ with (a) first- and second-neighbor pair, (b) first- through fourth-neighbor pair, and (c) first- through fourth-neighbor pair and triplet interactions. The squares and circles indicate the Monte Carlo results for $R(100)$ and $R(1\frac{1}{2}0)$, respectively. In (b) and (c), the interactions were chosen at random such that no interaction (except J_2) have magnitude greater than $0.2J_2$ and all interaction sets have as ground states either $L1_2$ or $D0_{22}$. The vertical solid (dashed) lines delineate $\langle 1\frac{1}{2}0\rangle$ from $\langle 100\rangle$ LRO (SRO).